Int J Biochem Mol Biol 2026;17(3):25-34
www.ijbmb.org /ISSN:2152-4114/IJBMB0170755

Original Article

Antimicrobial and antifungal efficacy of silver nanoparticles synthesized using *Xanthium strumarium* leaf extract

Arun Kumar Kashyap[1], Lalit Kumar Sahu[1], Priyadarsani Mishra[2], Khirabdhi Tanaya[3], Durgeshwer Singh[3], Nikita Kashyap[4], Buddhi Prakash Jain[2]

[1]*Department of Biotechnology, Govt. E Raghavendra Rao PG. Science College, Bilaspur 495006, C.G., India;* [2]*Gene Expression and Signaling Lab., Department of Zoology, Mahatma Gandhi Central University, Motihari, Bihar 845401, India;* [3]*Department of Botany, Mahatma Gandhi Central University, Motihari, Bihar 845401, India;* [4]*Department of ECE, Guru Ghasidas Vishwavidyalaya, Koni, Bilaspur 495009, C.G., India*

Received December 15, 2025; Accepted August 25, 2026; Epub August 25, 2026; Published August 30, 2026

Abstract: Introduction: Silver nanoparticles (AgNPs) are unique in their physical, chemical, and biological properties. AgNPs can be synthesized through several methods including chemical, physical, or biological. Due to eco-friendly approach and use of natural reducing agent, biological or green synthesis is more popular. Objective: The aim of the study is to synthesize silver nanoparticles (AgNPs) using *Xanthium strumarium* leaf extract, and explore their antimicrobial, and antifungal properties. Methods: UV-Visible spectroscopy and Transmission Electron Microscopy (TEM) was used for nanoparticles characterization. Antibacterial and antifungal activities of the synthesized nanoparticles were performed. Results: The bioactive compounds in the extract acted as natural reducing and stabilizing agents for AgNPs synthesis. The synthesized nanoparticles were confirmed by UV-Visible spectroscopy with a characteristic absorbance peak at 400-450 nm. Transmission Electron Microscopy (TEM) revealed spherical nanoparticles ranging from 10-100 nm with uniform size distribution. The synthesized AgNPs exhibited significant antibacterial activity against *Staphylococcus aureus* and *Escherichia coli*, as well as antifungal activity against *Aspergillus niger* and *Aspergillus fumigatus*. Conclusion: The study highlights the dual role of *Xanthium strumarium* as a synthesizing agent and a source of therapeutic potential, demonstrating its eco-friendly application in nanotechnology for biomedical and agricultural use.

Keywords: Silver nanoparticles, *Xanthium*, absorbance, anti-bacterial, anti-fungal

Introduction

Nanotechnology, which operates at the nanoscale (1-100 nm), has revolutionized various scientific and industrial fields due to its ability to manipulate materials at the atomic and molecular levels. Silver nanoparticles (AgNPs) are well known for their broad-spectrum antimicrobial activity, making them valuable for applications in medicine, pharmaceuticals, agriculture, and environmental science [1-3]. Nanoparticles play a significant role in drug delivery, tissue engineering, and diagnostics. Owing to their excellent optical properties and stability, they can be utilized in targeted drug delivery, wound dressings, body cements, and implants. They are used as imaging agents which help them with imaging of different body parts. Nanoparticles have the capability to stimulate the repair and growth of tissues and organs. Various nanoparticles have antimicrobial ability and thus, are used in antimicrobial wound dressings and medical devices. Nanoparticles can also be used in bioremediation to degrade pollutants such as heavy metals, dyes, etc. They are also used in agriculture as fertilisers and for delivery of pesticides, herbicides, etc. [4]. The synthesis of AgNPs can be achieved through physical, chemical, and biological methods. However, biological synthesis, also known as green synthesis, has emerged as a sustainable and eco-friendly alternative, avoiding the use of toxic chemicals and high energy requirements. Green synthesis utilizes natural

https://doi.org/10.62347/SDVI7410

resources such as plant extracts, microorganisms, or enzymes as reducing and stabilizing agents [2, 5]. While usage as a reducing agent, the electron in the compounds found in plant extract, carries out reduction of metals (M) such as Ag, Au, Pt etc. from bulk form (M^{x+}) to electric form (M^0). While the plant extract when used as a stabilizing agent, stabilizes the nanoparticles and protects them from arbitrary aggregations. They contain a repulsive force which controls the size and shape of the nanoparticles [6].

In the present study, *Xanthium strumarium*, commonly known as "chota gokhru" or "cocklebur", was employed for the green synthesis of silver nanoparticles. *Xanthium strumarium* have diverse therapeutic properties like anti-inflammation, anti-microbial activity, anti-oxidants etc. The phenolics, flavonoids, and alkaloids components of the plant act as reducing and capping agents for the synthesis of AgNPs. They play a crucial role in the reduction of ionic form into nano-form of metals such as Ag, Au, Pt, etc. [7]. Aerial parts of *Xanthium strumarium* contained many unidentified alkaloids, some sesquiterpene lactones such as xanthinin, xanthumin, xanthonol, xanthantin, xanthostrumarin, xanthonolides, atractyloside, etc. [8]. The leaf extract used in the study is known to contain approximately 24.7% of limonene and 10.6% of borneol. Thus, these compounds could have a role as a capping and reducing agent in the production of metallic nanoparticles [7]. They enable the environment-friendly reduction of silver ions to nanoscale silver without using hazardous chemical reagents [9]. This biological method utilizes the natural bioactive compounds of plants to effectively control the nucleation and stabilization of the resulting nanoparticles. Additionally, it may provide extra biological functions derived from the plant material [10]. To determine the size, shape, surface properties, crystallinity, and stability of AgNPs, various characterization techniques are employed. The position and shape of the peak in UV-Vis Spectroscopy provide insights into the size, shape, and aggregation of AgNPs. They exhibit a characteristic surface plasmon resonance (SPR) peak in the visible range, typically between 400 and 450 nm for spherical nanoparticles. Transmission Electron Microscopy (TEM) offers insights into the morphology, size, and structure of the synthesized AgNPs. The anti-bacterial activity of the synthesized nanoparticles against a range of bacterial species can be evaluated by the zone of inhibition method. Furthermore, the antifungal activity of the silver nanoparticles was also evaluated against various fungal strains, demonstrating significant inhibition. The antimicrobial mechanism of AgNPs is primarily attributed to their ability to release silver ions, which interact with microbial cell membranes, disrupt cellular components, and inhibit critical metabolic processes, leading to cell death [1, 2].

In the present work, we have synthesized silver nanoparticles using *Xanthium strumarium* leaf extract by green synthesis method, physicochemical characterization by UV-Visible spectrophotometer, and TEM methods, and their potent antimicrobial and antifungal properties. The AgNPs synthesized from the leaf extract of *Xanthium strumarium* have better stability and efficacy against microbes and fungus. The findings underscore the potential of AgNPs as eco-friendly and effective antimicrobial agents, with further research needed for their application in biomedical and environmental domains.

Material and methods

Sample collection and extract preparation

The fresh plant of *Xanthium strumarium* was collected from Khairi (22°05'28.6"N 81°57'01.1"E) village of Bilaspur district, Chhattisgarh. The plant has been verified, and its herbarium is preserved in the Department of Botany at Govt. E Raghavendra Rao P.G. Science College, Bilaspur, Chhattisgarh. After the sample collection, it was washed with tap water and air dried. The dried leaf sample was crushed into powder and stored for further experiments at room temperature.

In order to prepare leaf extract, the dried leaves were subjected to Soxhlet extraction by using methanol as a solvent. After extraction methanol was removed from the extract by using rota evaporator. The extract prepared was used for further analysis.

Silver nanoparticles synthesis

To prepare the stock solution, 10 mM solution of silver nitrate ($AgNO_3$ SRL, India) was made by dissolving 0.169 g of $AgNO_3$ in 100 mL of dis-

Table 1. Optimization of AgNPs synthesis using different concentrations of *Xanthium* leaf extract and silver nitrate solution

Sample Name	$AgNO_3$ Concentration (%)	Volume of $AgNO_3$ (mL)	*Xanthium* Extract Concentration (%)	Volume of Extract (mL)
XC1	0	0	100	40
XS1	10	4	90	36
XS2	20	8	80	32
XS3	30	12	70	28
XS4	40	16	60	24
XS5	50	20	50	20

tilled water, ensuring thorough mixing for complete dissolution. From this stock solution, 1 mM $AgNO_3$ solution was used for the synthesis of silver nanoparticles. Additionally, a 5% w/v of *Xanthium* dried leaf extract and distilled water was prepared by adding 10 g of dried *Xanthium* leaf powder to 200 mL of distilled water in a reagent bottle. The plant sample was treated at 60°C for 30 minutes. After cooling, the mixture was filtered through a Millipore filtration assembly to obtain a clear solution, and the final volume was adjusted to 200 mL. For synthesizing silver nanoparticles, reaction mixtures were put down into 40 mL dark bottles at various ratios of the 1 mM $AgNO_3$ solution and the 5% Xanthium plant extract, as tabulated in **Table 1**. The procedure requires combining the given volumes of the reagents in the dark bottles, and ensuring filling the bottles to the top for reduction and minimisation of air exposure. The prepared samples were heated at 60°C for 15 minutes. The bottles were then incubated at room temperature in darkness for 3-5 days to facilitate the synthesis of silver nanoparticles [11, 12]. The change of color may primarily indicate the formation of nanoparticles. Secondarily, the UV- Vis Spectrophotometer reading showing a peak in between 420-450 confirms the formation of nanoparticles.

UV-Vis spectrophotometry

The formation of silver nanoparticles was confirmed using UV-Vis spectrophotometry (Shimadzu UV-2600 240V EN Spectrophotometer (Shimadzu Corporation, Kyoto, Japan)). A spectrum scan was performed in the wavelength range of 350-700 nm. The characteristic surface plasmon resonance (SPR) peak in the range of 420-480 nm indicated the presence of silver nanoparticles [13, 14].

Transmission electron microscopy (TEM)

The morphological and structural characterization of the synthesized nanoparticles was conducted using Transmission Electron Microscopy (TEM). The TEM analysis was performed at the Center for Advanced Research, Dr. Harisingh Gour Central University, Sagar, India. A small amount of the nanoparticle suspension was drop-cast onto a carbon-coated copper grid and allowed to air-dry under ambient conditions before imaging. The grid was then loaded into the TEM instrument, and images were captured at various magnifications to study particle size, morphology, and aggregation patterns. High-resolution imaging was employed to analyze individual particle morphology, size and identify the degree of polydispersity in the sample [15].

Anti-bacterial activity

The bacterial culture of *Escherichia coli* (MTCC443) and *Staphylococcus aureus* (MTCC737) were obtained from the Department of Microbiology, D.L.S. PG. College, Bilaspur (C.G.). The culture was maintained on nutrient agar and refrigerated until further use. The bacterial cultures were recultured in nutrient broth media. Serial dilution was performed, 1 mL of the recultured nutrient media was added to 10 mL sterile distilled water and this method was carried out three times. The serially diluted sample was now at 10^{-3} dilution.

The Antimicrobial activity was tested using the Disc Diffusion Method, which operates on the principle of diffusion of antimicrobial agents from impregnated discs into an agar medium inoculated with bacterial strains. The 6 mm diameter discs were prepared from sterile filter paper infused with 100 ppm of silver nanoparticles (AgNPs). 1 mL of the serially diluted (10^{-3}) bacterial strains *Escherichia coli* (MTCC443) and *Staphylococcus aureus* (MTCC737) were inoculated on nutrient agar plates with the help of a spreader. The sterile filter paper discs soaked in known concentration of silver nanoparticle solution were placed on the surface, followed by incubation at 35°±2°C for 24 hours.

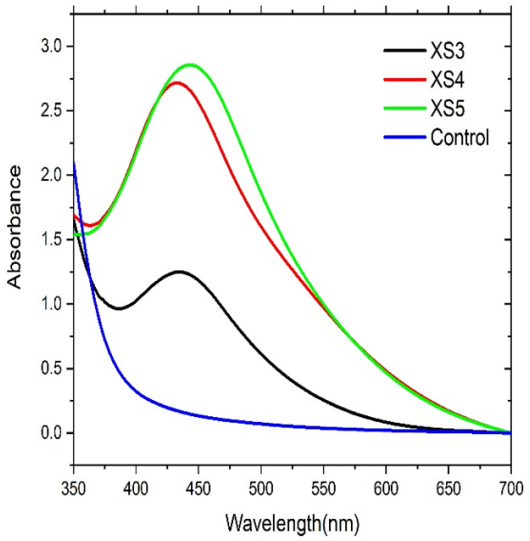

Figure 1. Absorbance of silver nanoparticles using UV-Vis spectroscopy: Absorbance vs Wavelength graph of samples (*XS*3, *XS*4 and *XS*5).

The experiment was performed on six different plates. Silver nanoparticles inhibit the growth of bacterial cells and form clear zones of inhibition around the discs. The experiment was performed on six replicates. The antimicrobial efficacy is directly proportional to the size of the inhibition zone against the tested bacteria.

Anti-fungal activity

39 g/L of Potato Dextrose Agar (PDA, SRL India) powder was dissolved in distilled water and then autoclaved. The antifungal effects of the synthesized silver nanoparticles (AgNPs) were evaluated on PDA plates with nutrient rich medium [16]. The plates were mixed with 500 µL of pre-prepared AgNPs solution and spread evenly on the plates. Fungal spores of strains (*Aspergillus* sps) were spread on the medium, and incubated at 25-28°C for 3-5 days to promote visible colony formation [17]. Different fungal strains were tested on the separate plates to avoid cross-contamination. After incubation at 25-28°C, the fungal growth were observed for 3 days [18].

Statistical analysis

The results obtained from carrying out the antibacterial activity were statistically analysed using GraphPad Prism (Version 8.0.2 (263)). The experimental value from six independent sets were taken as input, and analysed Shapiro-Wilk test to test the normal distribution of data. Kruskal-Wallis test was applied on non-normal distributed datasets. Further, post hoc test (Dunn's Multiple Comparison Test) was applied to show which group differs. Data were represented as median (range) for each group. The *p* value significance was obtained for Kruskal-Wallis test. All data were analysed by non-parametric methods. *P* value < 0.05 was considered statistically significant.

Results

Biological synthesis and characterization of Silver Nanoparticles using Xanthium leaf extract

Silver nanoparticles are synthesized using leaf extract from *Xanthium* as a reducing agent. A color change from pale yellow to muddy brown in the solution indicates the formation of silver nanoparticles in samples XS3, XS4 and XS5. This change is caused by the reduction of silver ions, which leads to the creation of silver nanoparticles. The formation of the silver nanoparticles was determined using UV-Vis absorption spectroscopy. The absorption spectra of silver nanoparticle samples XS3, XS4 and XS5 were analyzed to confirm nanoparticle synthesis and evaluate their properties. All nanoparticle samples displayed distinct absorbance peaks between 420 and 450 nm (**Figure 1**), a characteristic feature of silver nanoparticles. No absorbance was shown by control sample, which confirm the absence of any nanoparticles in the control samples. The sample number XS5 showed the highest absorbance peaks at approximately 440-460 nm, while XS3 exhibited lower peaks. The difference in the absorbance is due to differences in nanoparticle concentration or size.

Size determination of silver nanoparticles

The TEM analysis of nanoparticles, which was synthesized by using *Xanthium strumarium* (XS5) extract displayed explicit structural and morphological characteristics. At lower magnifications (200 nm scales), the nanoparticles predominantly showed agglomerated clusters, establishing branched and irregularly shaped assemblies. This aggregation results strong inter-particle interactions, that happens poten-

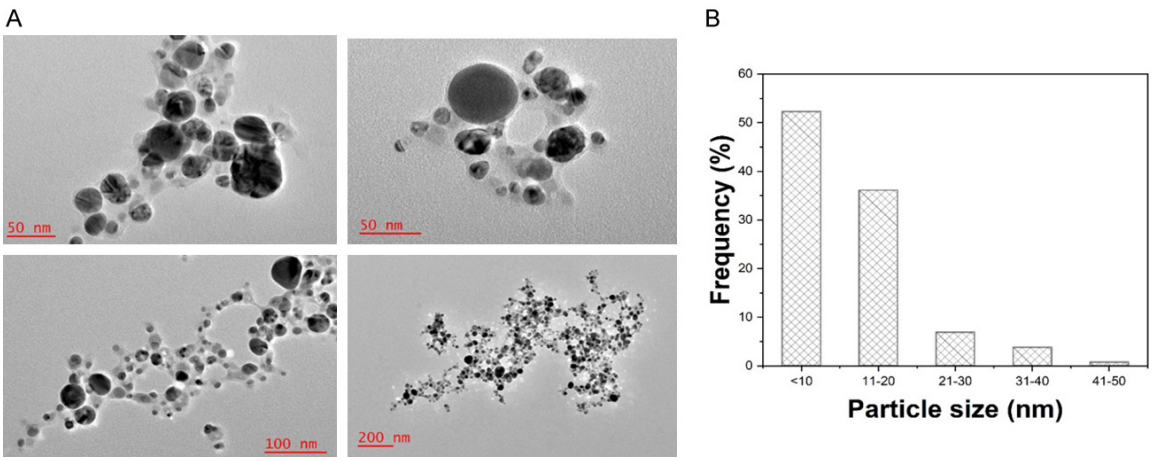

Figure 2. Morphological and size distribution analysis of synthesized silver nanoparticles. A. TEM Image; B. Particle Size Histogram.

Table 2. Zone of inhibition test for *Staphylococcus aureus* and *Escherichia coli*

Sample	Zone of Inhibition (in mm)	
	Staphylococcus aureus	*Escherichia coli*
Control	0	0
XS4	11 (8-12)	13 (12-16)
XS5	13 (10-16)	15 (14-16)

Values are represented as Median (range).

tially due to van der Waals forces or insufficient stabilization during the synthesis process. The elaborated visualization at higher magnification (10 nm, 50 nm, and 100 nm scales) displayed primarily spherical morphology (**Figure 2A**). The image confers a histogram depicting the particle size distribution derived from TEM data as shown in **Figure 2B**. In further analysis of the images, it was observed that approximately 52% of the particles are smaller than 10 nm, whereas less than 1% while less than 1% fall within the 41-50 nm range. This data shows a clear preference for smaller particle sizes, with approximately 88% of the particles measuring below 20 nm. Such size distribution confirms that the synthesis of AgNPs was characterized by controlled nucleation and growth.

Anti-bacterial activity of synthesised silver nanoparticles

The Antimicrobial efficiency of silver nanoparticles synthesised from *Xanthium* plant extract was evaluated using the Disc Diffusion method. The zone of inhibition was measured. The cultures of *Escherichia coli* and *Staphylococcus aureus* were used as test organisms. Nanoparticles were synthesised in three variants: XS3, XS4, and XS5. The Sample XS3 exhibited broader peaks, and XS4, XS5 showed a narrower peak. Thus, the samples XS4 and XS5 were chosen for testing the antibacterial activity of the sample. No positive control (antibiotic) was used as the antibacterial properties of silver nanoparticles are well known and have been extensively reported. The negative control, which contained no nanoparticles, was used. The Zone of Inhibition was measured for XS4 and XS5 samples. Zone of inhibition (in mm) upon silver nanoparticle treatment against *Staphylococcus aureus* and *Escherichia coli* is shown is Supplementary Table 1. In the case of *Escherichia coli*, both samples XS4 and XS5 showed a zone of inhibition of 13 (12-16) mm and 15 (14-16) mm, respectively. In the case of *Staphylococcus aureus*, both XS4 and XS5 showed a zone of inhibition of 11 (8-12) mm and 13 (10-16) mm, respectively (**Table 2**). Values are represented as median (range). The control sample, lacking nanoparticles, showed no antibacterial effects, confirming that the observed inhibition zones in the nanoparticle samples were due to the presence of AgNPs (**Figure 3**). The silver nanoparticles produced showed slightly better antimicrobial properties towards Gram-negative *Escherichia coli* than Gram-positive *Staphylococcus aureus*. The results were statistically analysed and the *p*-value significance was obtained. For, the test of normality against the

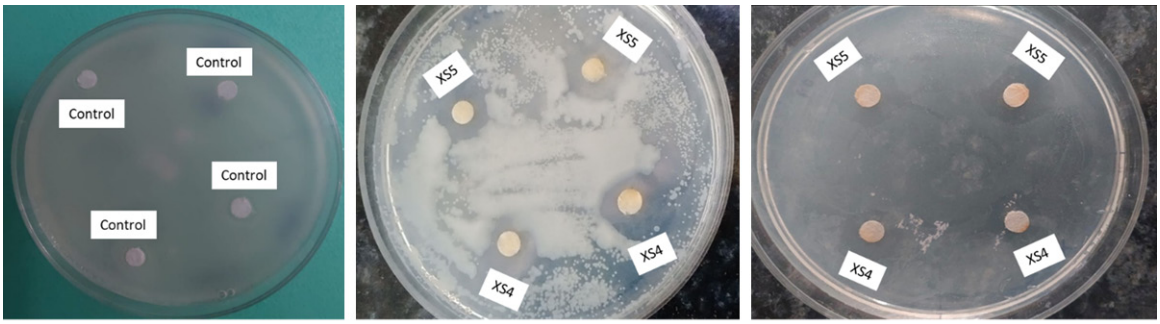

Figure 3. Zone of inhibition of gram-positive bacteria and gram-negative bacteria.

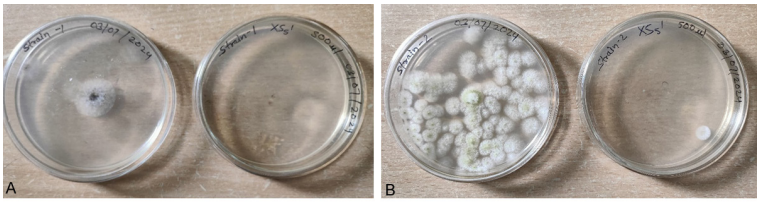

Aspergillus niger (Strain 1) *Aspergillus fumigatus* (Strain 2)

Figure 4. Antifungal activity of XS5 towards two fungal strains, Aspergillus niger (Strain 1) and Aspergillus fumigatus (Strain 2). (A) Aspergillus niger and (B) Aspergillus fumigatus. Left: Control; Right: XS5 treatment.

Shapiro-Wilk test, *p*-value for XS4 and XS5 for *Staphylococcus aureus* 0.0911 and 0.1911 respectively, while for *Escherichia coli* it was 0.0347 and 0.004 respectively (Supplementary Table 2). Since some of the data significantly deviated from normality; therefore, non-parametric test (Kruskal-Wallis) was employed. As shown in Supplementary Table 3, *p* value is less than 0.05 (0.0004), the Kruskal-Wallis test showed significant differences among groups. Further Dunn's multiple comparisons test was applied for pairwise comparison. The results are represented in Supplementary Table 4.

Anti-fungal activity of synthesised silver nanoparticles

The antifungal activity of XS5 silver nanoparticles (AgNPs) was evaluated against two fungal strains, *Aspergillus niger* (Strain 1) and *Aspergillus fumigatus* (Strain 2), by spreading the nanoparticles evenly across Potato Dextrose Agar (PDA) plates. In the control plates, where no AgNPs were applied, both fungal strains exhibited normal growth. For *Aspergillus niger*, significant inhibition of growth was observed on the AgNP-treated plates, indicating the effective anti-fungal properties of the nanoparticles. Similarly, *Aspergillus fumigatus* (**Figure 4**) showed minimal or no growth on the AgNP-treated plates, while the control plates allowed unrestricted fungal growth, confirming the inhibitory effect of XS5 AgNPs.

Shelf-life evaluation of silver nanoparticles

The UV-Vis spectrophotometric technique was applied to confirm the stability of silver nanoparticles. The absorption spectrum of the silver nanoparticle samples stored for 6 and 12 months was recorded (**Figure 5**). The UV-Vis analysis of the silver nanoparticles (0 day) shows an absorption band around 420 nm, which corresponds to the surface plasmon resonance absorption band of silver nanoparticles. The UV-Vis absorption spectra of the silver nanoparticles samples taken after 6 months of storage show the absorption maxima at 430 nm, which is very close to the initial peak position indicating no agglomeration of silver nanoparticles. Absorption spectra of the samples measured after storage for 12 months also show no significant change in the spectral shape or the intensity, indicating that the silver nanoparticles are stable over a period of 12 months. The absorption spectra of the silver nanoparticles, recorded immediately after the preparation and up to 12 months confirmed the very good stability of the samples. The unchanged peak shape and position indicate

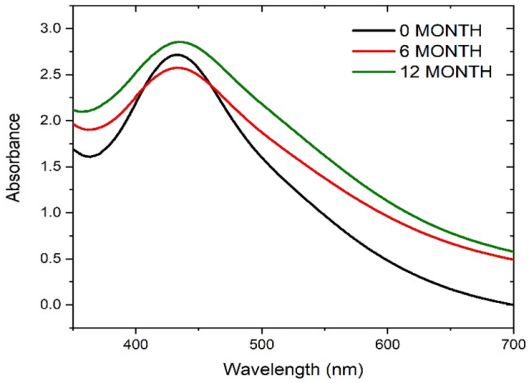

Figure 5. UV-Vis spectra of synthesized AgNPs stored over time.

no change in the size of the particles, or an occurrence of their agglomeration.

Discussion

The SPR peak between 400 to 450 nm in UV-Vis spectra highlighted the successful formation of silver nanoparticles [19]. The variations in peak intensity and position among the samples occurs due to differences in the concentration, size, and nanoparticles distribution, and also influenced by the different synthesis conditions. The distinct absorbance peaks for XS5 is due to higher concentration, well-dispersed, and spherical shape of AgNPs, while the lower peaks for XS3 might be due to a low concentration, incomplete synthesis, aggregation and possible impurities [1]. Nanoparticle properties are dependent on the synthesis conditions and precise control leads to the desired nanoparticle characteristics [20].

TEM was used to verify the morphology and size characteristics of the AgNPs. The TEM micrographs indicated that the silver nanoparticles in the present study are spherical in shape. Around 88% of the particles are smaller than 20 nm as evident in the TEM images. Some aggregation is observed at lower magnifications. The possible reasons for aggregation during green synthesis approach are inadequate capping agents, surface energy minimization, change in pH, temperature, ionic strength etc. [21]. Additional stabilizing agents could significantly reduce aggregation and enhance the colloidal stability of the nanoparticles [22]. Further refinement in the size and distributions in the nanoparticles are required for potential applications in areas such as catalysis, biomedicine, and environmental remediation [23, 24].

The synthesized nanoparticles showed significant antibacterial as well as anti-fungal properties. Since no zone of inhibition was observed during anti-bacterial assay, which confirm the efficacy and activities of the nanoparticles against bacterial strains. The variation in the size of zone of inhibition with different samples of nanoparticles are due to their different size, concentration, and surface properties, which influence their interaction with bacterial cells [2, 25, 26]. Among the different nanoparticle samples, XS5 showed a strong antibacterial effect on *Staphylococcus aureus* and *Escherichia coli,* which may be due to its higher nanoparticle concentration or optimal size distribution. Conversely, XS4 weaker activity results from a lower concentration or less effective nanoparticle structure. These results indicate a higher concentration of $AgNO_3$ showed the presence of a higher concentration of nanoparticles than other lower concentrations and thus, showed better antibacterial activity. The comparable effectiveness of XS4 and XS5 against different strains of bacteria highlights the reproducibility of the synthesis conditions for achieving potent antibacterial properties [27-29]. Silver nanoparticles (AgNPs) are known to exhibit antibacterial activity against both Gram-negative and Gram-positive bacteria [1, 27]. However, Gram-negative bacteria *(E. coli),* which have a thinner peptidoglycan layer and an outer membrane, have greater susceptibility to AgNPs compared to Gram-positive bacteria (*S. aureus*), which have thicker peptidoglycan layers. The increased effectiveness against Gram-negative bacteria makes AgNPs promising for treating multidrug-resistant infections caused by pathogens like *E. coli* and *P. aeruginosa*, whereas higher concentrations are usually necessary for similar inhibition of Gram-positive species such as *S. aureus*. Crisan et al. 2024 carried out the antibacterial activity of silver nanoparticles in two different concentrations (10 µg/ml and 100 µg/ml) against *S. aureus* and *E. coli* via well diffusion method. They found that 10 µg/ml showed a zone of inhibition (ZOI) of 9.3±1.034 mm and 100 µg/ml showed a ZOI of 14±1.577 mm in case of *S. aureus* whereas 10 µg/ml showed a zone of inhibition (ZOI) of 11±0.00

mm and 100 µg/ml showed a ZOI of 12.57± 0.88 mm in case of *E. coli*. This data shows a similar trend when compared to our results [30]. Tessema et al. 2024 evaluated the antibacterial activity of silver nanoparticles (AgNPs) and modified silica gel containing AgNPs. They found the maximum zone of inhibition among various concentrations of AgNPs against *E. coli* and *S. aureus* to be 12.80 mm and 14.30 mm respectively which aligns with the results found in this study [31]. In another study the antibacterial activity of AgNPs against *E. coli* was evaluated and found results that align with the study. He found that *E. coli* showed a zone of inhibition of 14.5±1.1 mm, which was the range found in this study [32].

Nanoparticles synthesis conditions, size and their activity against specific bacterial strains for better efficacy can be explored in further analysis [29]. Sample XS5 exhibited strong anti-fungal properties against the known strain of *Aspergillus niger* and *Aspergillus fumigatus*. Decreased fungal growth upon treatment with synthesized nanoparticles in comparison to the control plates features the nanoparticles' ability to interfere with fungal cell structures and metabolic functions. AgNPs cause disruption to the fungal cell membranes, hamper the intracellular components, and generate reactive oxygen species (ROS), which are collectively responsible for inhibiting the fungal growth [33, 34]. The significant inhibition of *Aspergillus niger* suggests that XS5 AgNPs targets the mechanisms that are involved in the growth of the organism and almost complete inhibition of *Aspergillus fumigatus* demonstrates the broad-spectrum inhibitory potential of the nanoparticles [34]. The unhindered growth on the control plates' confirms the inhibitory effects are because of the presence of AgNPs. AgNPs are uniformly distributed across the growth medium, which enhances the antifungal effectiveness by ensuring thorough contact between the nanoparticles and fungal spores or mycelia [10, 33]. The study confirms the potentiality of XS5 AgNPs as an effective antifungal agent against pathogenic strains such as *A. niger* and *A. fumigatus*. Future work could involve optimizing the nanoparticle concentration and exploring the mechanism of action in detail to further enhance their antifungal efficacy for applications in agriculture, healthcare, and food preservation [34, 35].

Conclusion

This study demonstrates the successful green synthesis of silver nanoparticles (AgNPs) using *Xanthium strumarium* leaf extract. The synthesized AgNPs were initially characterized by UV-Vis spectroscopy, and then Transmission Electron Microscopy (TEM) was used to confirm their formation, size distribution, and morphology. The synthesized nanoparticles showed significant antimicrobial activity against Gram-positive and Gram-negative bacteria, alongside promising antifungal properties. The eco-friendly synthesis approach employed in this study underscores the potential of plant-based methods for producing biocompatible and cost-effective silver nanoparticles. The synthesized nanoparticles from *Xanthium strumarium* after further characterization and additional experimentation, can be used as potent antimicrobial and antifungal agents. Further optimization of the synthesis process and detailed mechanistic studies can enhance the stability and efficacy of these nanoparticles, contributing to the development of sustainable nanotechnology-based solutions for global challenges.

Acknowledgements

We acknowledge Mahatma Gandhi Central University Motihari and Govt. E. Raghvendra Rao P.G. Science College Bilaspur to carry out this work.

Disclosure of conflict of interest

None.

Address correspondence to: Buddhi Prakash Jain, Gene Expression and Signaling Lab., Department of Zoology, Mahatma Gandhi Central University, Motihari, Bihar 845401, India. E-mail: buddhiprakash@mgcub.ac.in; Durgeshwer Singh, Department of Botany, Mahatma Gandhi Central University, Motihari, Bihar 845401, India. E-mail: durgeshwersingh@mgcub.ac.in; Arun Kumar Kashyap, Department of Biotechnology, Govt. E Raghavendra Rao PG. Science College, Bilaspur 495006, C.G., India. E-mail: akkbiotech@gmail.com

References

[1] Singh S, Bharti A and Meena VK. Green synthesis of multi-shaped silver nanoparticles: optical, morphological and antibacterial prop-

erties. J Mater Sci Mater Electron 2015; 26: 3638-48.
[2] Ying S, Guan Z, Ofoegbu PC, Clubb P, Rico C, He F and Hong J. Green synthesis of nanoparticles: current developments and limitations. Environ Technol Innov 2022; 26: 102336.
[3] Gupta D, Boora A, Thakur A and Gupta TK. Green and sustainable synthesis of nanomaterials: recent advancements and limitations. Environ Res 2023; 231: 116316.
[4] Altammar KA. A review on nanoparticles: characteristics, synthesis, applications, and challenges. Front Microbiol 2023; 14: 1155622.
[5] Hano C and Abbasi BH. Plant-based green synthesis of nanoparticles: production, characterization and applications. Biomolecules 2021; 12: 31.
[6] Patra D and El Kurdi R. Curcumin as a novel reducing and stabilizing agent for the green synthesis of metallic nanoparticles. Green Chem Lett Rev 2021; 14: 474-87.
[7] Kumar PV, Jelastin Kala SM and Prakash KS. Green synthesis derived Pt-nanoparticles using Xanthium strumarium leaf extract and their biological studies. J Environ Chem Eng 2019; 7: 103146.
[8] Kamboj A and Saluja A. Phytopharmacological review of Xanthium strumarium L. (Cocklebur). Int J Green Pharm 2010; 4: 129.
[9] Kashyap AK, Bisoyi P and Jain BP. Antioxidant, anti-microbial, anti-inflammatory and cytotoxic effect of macrotyloma uniflorum leaf extract. Adv Pharmacol Pharm 2023; 11: 179-86.
[10] Devi JS and Bhimba BV. Antibacterial and antifungal activity of silver nanoparticles synthesized using hypnea muciformis. Biosci Biotechnol Res Asia 2014; 11.
[11] Pungle R, Nile SH, Makwana N, Singh R, Singh RP and Kharat AS. Green synthesis of silver nanoparticles using the *Tridax procumbens* plant extract and screening of its antimicrobial and anticancer activities. Oxid Med Cell Longev 2022; 2022: 9671594.
[12] Asif M, Yasmin R, Asif R, Ambreen A, Mustafa M and Umbreen S. Green synthesis of silver nanoparticles (AgNPs), structural characterization, and their antibacterial potential. Dose Response 2022; 20: 15593258221088709.
[13] Khodashenas B and Ghorbani HR. Synthesis of silver nanoparticles with different shapes. Arab J Chem 2019; 12: 1823-38.
[14] Nguyen NPU, Dang NT, Doan L and Nguyen TTH. Synthesis of silver nanoparticles: from conventional to 'modern' methods-a review. Processes 2023; 11: 2617.
[15] Malatesta M. Transmission electron microscopy as a powerful tool to investigate the interaction of nanoparticles with subcellular structures. Int J Mol Sci 2021; 22: 12789.
[16] Gibała A, Żeliszewska P, Gosiewski T, Krawczyk A, Duraczyńska D, Szaleniec J, Szaleniec M and Oćwieja M. Antibacterial and antifungal properties of silver nanoparticles-effect of a surface-stabilizing agent. Biomolecules 2021; 11: 1481.
[17] Matras E, Gorczyca A, Przemieniecki SW and Oćwieja M. Surface properties-dependent antifungal activity of silver nanoparticles. Sci Rep 2022; 12: 18046.
[18] El Badawy AM, Luxton TP, Silva RG, Scheckel KG, Suidan MT and Tolaymat TM. Impact of environmental conditions (pH, ionic strength, and electrolyte type) on the surface charge and aggregation of silver nanoparticles suspensions. Environ Sci Technol 2010; 44: 1260-6.
[19] Fu LM, Hsu JH, Shih MK, Hsieh CW, Ju WJ, Chen YW, Lee BH and Hou CY. Process optimization of silver nanoparticle synthesis and its application in mercury detection. Micromachines (Basel) 2021; 12: 1123.
[20] Agustina TE, Handayani W and Imawan C. The UV-VIS spectrum analysis from silver nanoparticles synthesized using Diospyros maritima Blume. Leaves extract 3rd KOBI congress, international and national conferences (KOBICINC 2020). Atlantis Press 2021; 411-9.
[21] Sati A, Ranade TN, Mali SN, Ahmad Yasin HK and Pratap A. Silver nanoparticles (AgNPs): comprehensive insights into bio/synthesis, key influencing factors, multifaceted applications, and toxicity-a 2024 update. ACS Omega 2025; 10: 7549-82.
[22] Haiouani K, Hegazy S, Alsaeedi H, Bechelany M and Barhoum A. Green synthesis of hexagonal-like ZnO nanoparticles modified with phytochemicals of clove (Syzygium aromaticum) and thymus capitatus extracts: enhanced antibacterial, antifungal, and antioxidant activities. Materials (Basel) 2024; 17: 4340.
[23] Michen B, Geers C, Vanhecke D, Endes C, Rothen-Rutishauser B, Balog S and Petri-Fink A. Avoiding drying-artifacts in transmission electron microscopy: characterizing the size and colloidal state of nanoparticles. Sci Rep 2015; 5: 9793.
[24] Sidhu AK, Verma N and Kaushal P. Role of biogenic capping agents in the synthesis of metallic nanoparticles and evaluation of their therapeutic potential. Front Nanotechnol 2022; 3.
[25] Loo YY, Rukayadi Y, Nor-Khaizura MA, Kuan CH, Chieng BW, Nishibuchi M and Radu S. In vitro antimicrobial activity of green synthesized silver nanoparticles against selected gram-negative foodborne pathogens. Front Microbiol 2018; 9: 1555.
[26] Menichetti A, Mavridi-Printezi A, Mordini D and Montalti M. Effect of size, shape and surface functionalization on the antibacterial activity of

silver nanoparticles. J Funct Biomater 2023; 14: 244.
[27] Bruna T, Maldonado-Bravo F, Jara P and Caro N. Silver nanoparticles and their antibacterial applications. Int J Mol Sci 2021; 22: 7202.
[28] Urnukhsaikhan E, Bold BE, Gunbileg A, Sukhbaatar N and Mishig-Ochir T. Antibacterial activity and characteristics of silver nanoparticles biosynthesized from Carduus crispus. Sci Rep 2021; 11: 21047.
[29] Rodrigues AS, Batista JGS, Rodrigues MÁV, Thipe VC, Minarini LAR, Lopes PS and Lugão AB. Advances in silver nanoparticles: a comprehensive review on their potential as antimicrobial agents and their mechanisms of action elucidated by proteomics. Front Microbiol 2024; 15: 1440065.
[30] Crisan MC, Pandrea SL, Matros L, Mocan T and Mocan L. In vitro antimicrobial activity of silver nanoparticles against selected Gram-negative and Gram-positive pathogens. Med Pharm Rep 2024; 97: 280-97.
[31] Tessema B, Gonfa G, Mekuria Hailegiorgis S, Workneh GA and Getachew Tadesse T. Synthesis and evaluation of the anti-bacterial effect of modified silica gel supported silver nanoparticles on *E. coli* and *S. aureus*. Results Chem 2024; 7: 101471.
[32] Abdulraof LAA and Naser HH. Synergistic antimicrobial activity of a novel synthetic peptide and silver nanoparticles against multidrug-resistant E. coli. Int J Environ Sci 2025; 11: 828-53.
[33] Li L, Pan H, Deng L, Qian G, Wang Z, Li W and Zhong C. The antifungal activity and mechanism of silver nanoparticles against four pathogens causing kiwifruit post-harvest rot. Front Microbiol 2022; 13: 988633.
[34] Hashem AH, Saied E, Amin BH, Alotibi FO, Al-Askar AA, Arishi AA, Elkady FM and Elbahnasawy MA. Antifungal activity of biosynthesized silver nanoparticles (AgNPs) against aspergilli causing aspergillosis: ultrastructure study. J Funct Biomater 2022; 13: 242.
[35] Górka K and Kubiński K. Antifungal activity against human and plant mycopathogens, and green synthesis of silver nanoparticles exhibiting such activity. Appl Sci 2024; 14: 115.

Supplementary Table 1. Zone of inhibition (in mm) upon silver nanoparticle treatment against *Staphylococcus aureus* and *Escherichia coli*

Control	*Staphylococcus aureus*		*Escherichia coli*	
	XS4	XS5	XS4	XS5
0	12	16	14	16
0	12	16	16	16
0	12	14	16	16
0	10	12	12	14
0	10	10	12	14
0	8	10	12	14

Supplementary Table 2. Test for normal distribution: Shapiro-Wilk test

Control	Input	*Staphylococcus aureus*		*Escherichia coli*	
		XS4	XS5	XS4	XS5
W		0.8216	0.8606	0.7752	0.6827
P value		0.0911	0.1912	0.0347	0.004
Passed normality test (alpha=0.05)?		Yes	Yes	No	No
P value summary		ns	ns	*	**
Number of values	6	6	6	6	6

ns, not significant; *, P < 0.05; **, P < 0.01.

Supplementary Table 3. Kruskal wallis test

Kruskal wallis test	
P value	0.0004
Exact or approximate *P* value?	Approximate
P value summary	***
Do the medians vary signif. (P < 0.05)?	Yes
Number of groups	5
Kruskal-Wallis statistic	20.72

***, P < 0.001.

Supplementary Table 4. Dunn's multiple comparisons test

Dunn's multiple comparisons test	Mean rank diff.	Significant?	Summary	Adjusted *P* Value
control vs. XS4 E	-16.5	Yes	**	0.0093
control vs. XS4 S	-8.333	No	ns	0.9436
control vs. XS5 E	-20.5	Yes	***	0.0004
control vs. XS5 S	-14.67	Yes	*	0.0324
XS4 E vs. XS4 S	8.167	No	ns	>0.9999
XS4 E vs. XS5 E	-4	No	ns	>0.9999
XS4 E vs. XS5 S	1.833	No	ns	>0.9999
XS4 S vs. XS5 E	-12.17	No	ns	0.1459
XS4 S vs. XS5 S	-6.333	No	ns	>0.9999
XS5 E vs. XS5 S	5.833	No	ns	>0.9999

ns, not significant; *, P < 0.05; **, P < 0.01; ***, P < 0.001.